

Radar-Derived Insights of Microphysical Processes

Using the NSF NCAR S-Pol Radar

Ian Cornejo^a, Angela Rowe^a, Michael Bell^b, Wei-Yu Chang^c
^aUniversity of Wisconsin – Madison, ^bColorado State University, ^cNational Central University



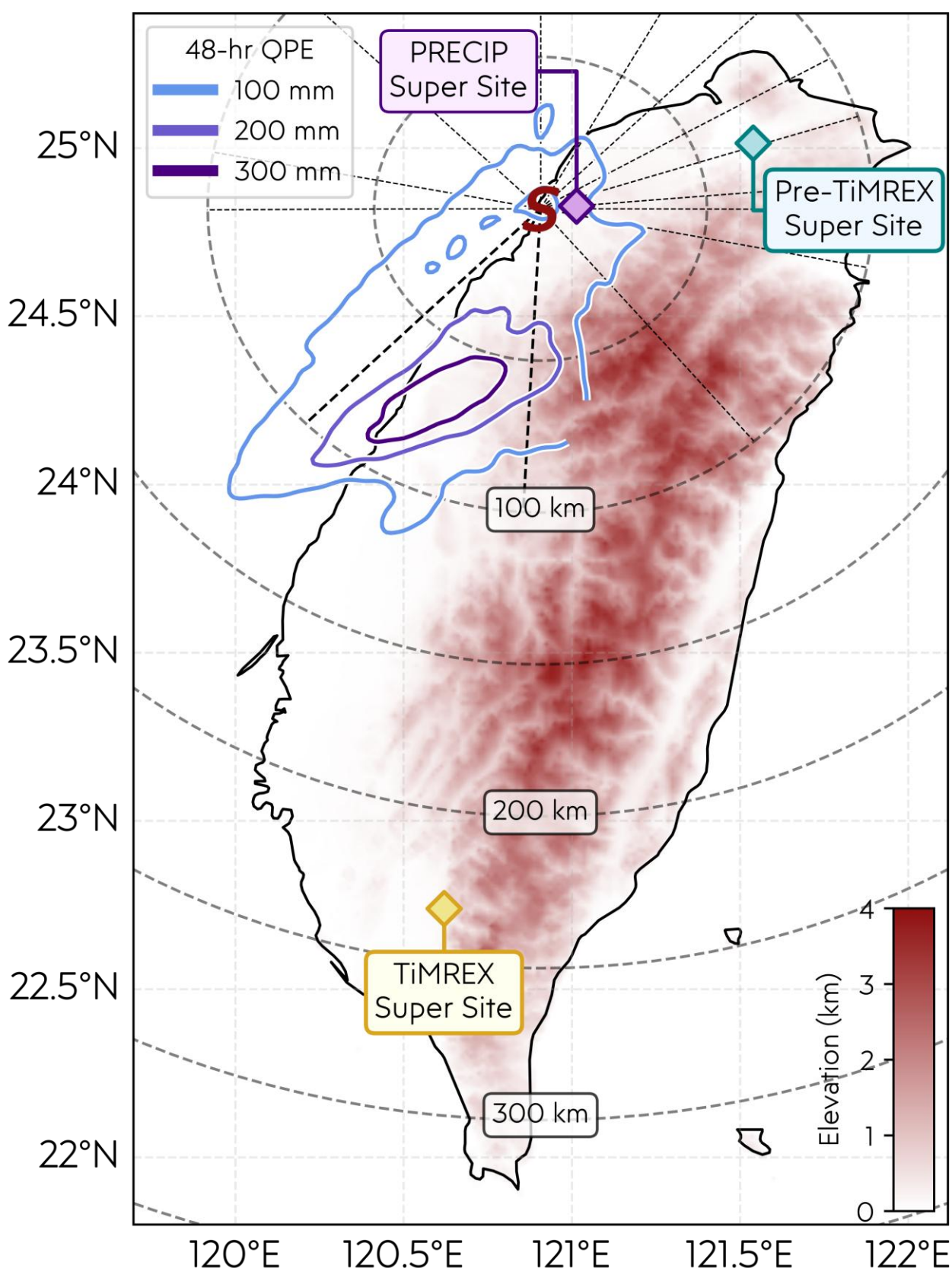
Introduction

- Better understanding of the **microphysical processes** that lead to **extreme rainfall near complex terrain** is needed.
- The PRECIP 2022 field campaign in Taiwan studied heavy rainfall, including IOP 1 Mei-Yu case with **>300 mm of rainfall in 48-h** (Fig. 1)

What are the dominant microphysical processes that contribute to convective Mei-Yu rainfall near terrain?

- Objective:** Model the **Drop Size Distribution (DSD)** from **NSF NCAR S-Pol**, including lower-order moments, to link to microphysical inferences and rainfall.

Figure 1: Elevation Map with super site locations and S-Pol (S) range rings, RHs, and 48-h OPE (contours)



Modeling DSDs

- Training Dataset:** Micro Rain Radars and 2-D Video Disdrometers from 2008 Pre-TIMREX and TIMREX combined to create full DSDs (Fig. 1).
- Model:** Generalized-Gamma (GG) fitted **Double-Moment Normalized DSD**^[1].
- Normalization Moments and Inputs to the Model:** A novel $M_3(A_h, Z_{dr})$ retrieval and $M_6(Z_h)$, with A_h retrieval for S-Pol described in Cornejo et al. (2025)^[2].
- Model Fitting:** The **MRR+2DVD** median normalized DSD, $h(x)$, is similar to the **GG US Fit**, while capturing smaller normalized diameters, x , unlike **2DVD** alone (Fig. 2).
- Performance:** When applied to S-Pol, the **model performs well** compared to a **PRECIP PARSIVEL** (Fig. 3). Additional quality control checks removed suspect model output.
- Gridding:** M_3 retrieval and DSD model applied to **14 S-Pol RHs** (Fig. 1), gridded using **DAISHO** ($\Delta x = \Delta z = 250$ m), and with echo partitioning from **ECCO**^[3].

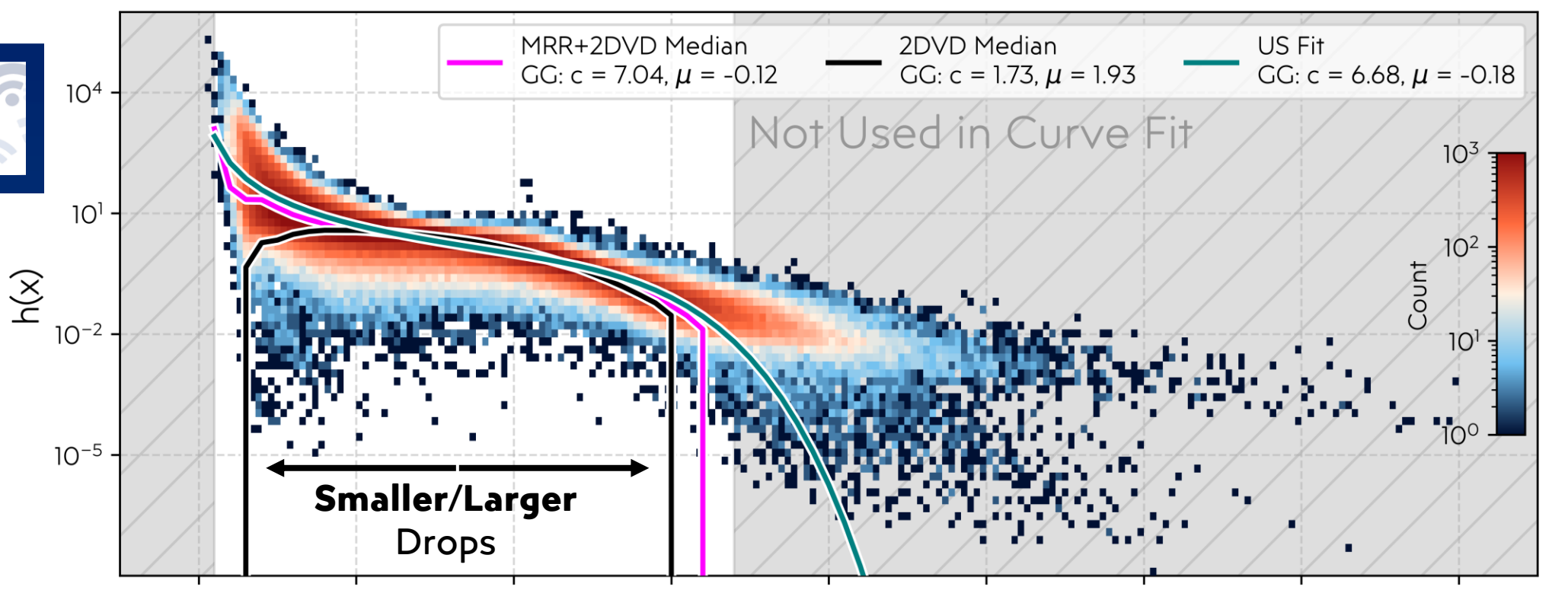
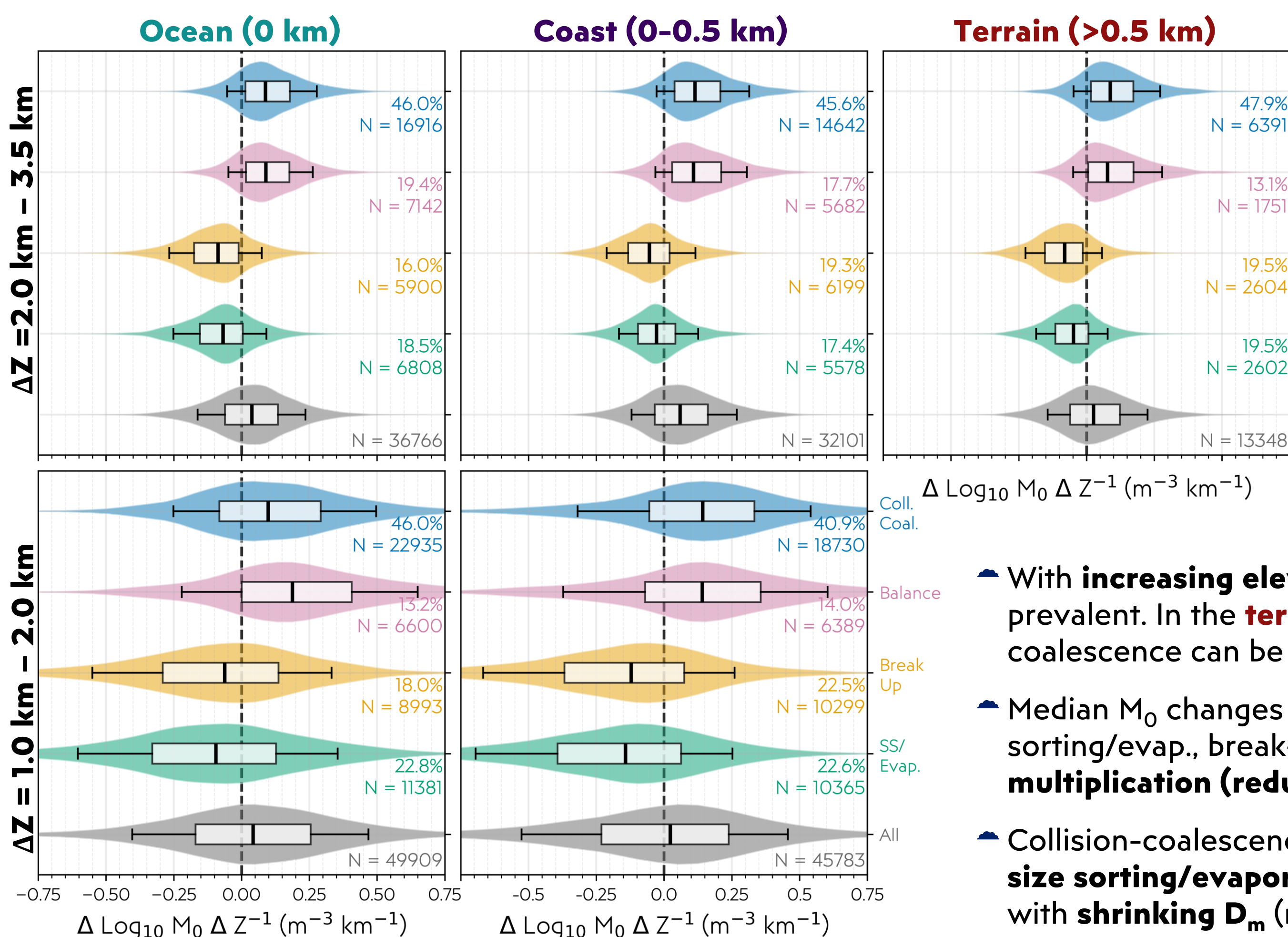


Figure 2: Normalized drop concentration using the combined **MRR+2DVD** dataset with a median fit, a median fit if only using the **2DVD**, and the **US Fit**.

Integrating Modeled DSDs with Warm Rain Inferences



- Microphysical **Fingerprints**^[4] are supported with **modeled M_0** (# of drops) for **convection** during PRECIP IOP 1 (Fig. 4).
- The most frequently occurring, dominant process aloft and near the surface is **collision-coalescence** with greater variability among processes nearest the surface.

- With **increasing elevation**, drop break-up is more prevalent. In the **terrain**, reduced low-level collision coalescence can be inferred.
- Median M_0 changes show collision-coalescence (size sorting/evap., break-up) is coincident with **drop multiplication (reduction)**.
- Collision-coalescence associated with D_m growth whereas **size sorting/evaporation and break-up** are associated with **shrinking D_m** (not shown).

Figure 4: Distributions of depth-normalized change in M_0 for different inferred microphysical processes (i.e., fingerprint) over defined altitude ranges. Elevation and altitude relative frequency of occurrence for each fingerprint is provided as a percentage.

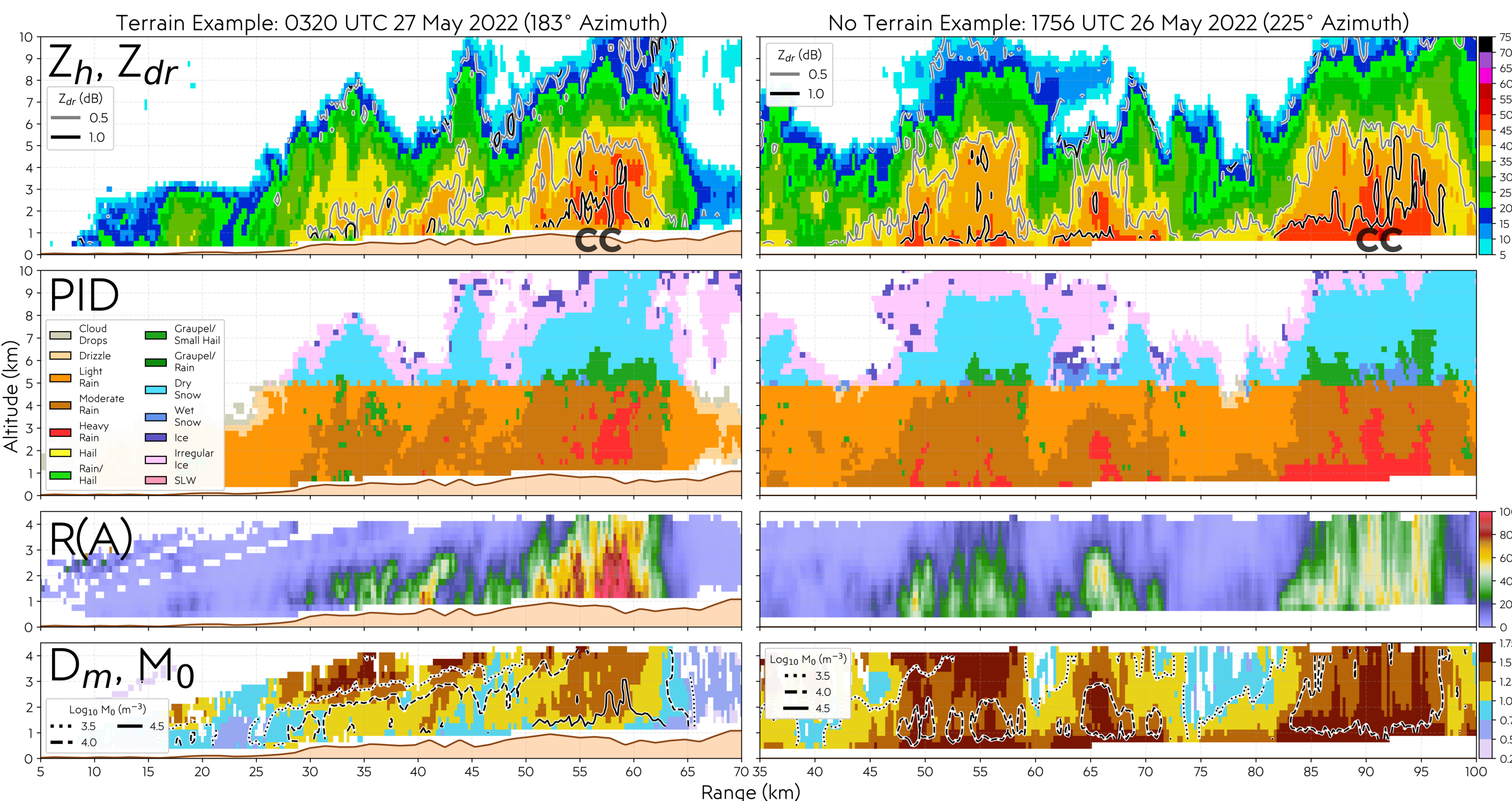


Figure 5: Gridded RHs from S-Pol at the 183° azimuth (left) and 225° azimuth (right) using Z_{dr} with contoured Z_h , PID, Rain Rate from A_h , and modeled D_m with contoured M_0 . CC indicates region of inferred collision coalescence.

- In both a terrain and no terrain example (Fig. 5), we find **inferred collision coalescence** (increasing Z_h/Z_{dr} towards the surface; **CC** on figure) in convection.
- Similar PID signatures** are found in collision coalescence:
 - Graupel** above the melting layer.
 - Transition into **Moderate Rain** below the melting layer.
 - Growth into **Heavy Rain** near the surface.
- However, the **terrain example exhibits greater rain rates using A_h** despite higher Z_h at the surface in the no terrain example.
- Modeled moments show differences despite similar CC:**
 - Similar D_m** below the melting layer, but **D_m shrinking (growth)** found in **Terrain (No Terrain)** example.
 - Greater M_0 below the melting layer in terrain example**, but the **D_m shrinking** below is coincident with drop multiplication (**increasing M_0**). No terrain example does **not see much M_0 change**.
- A control on rain rate seems to be **M_0 just below the melting layer** suggesting that **ice processes** should be investigated.

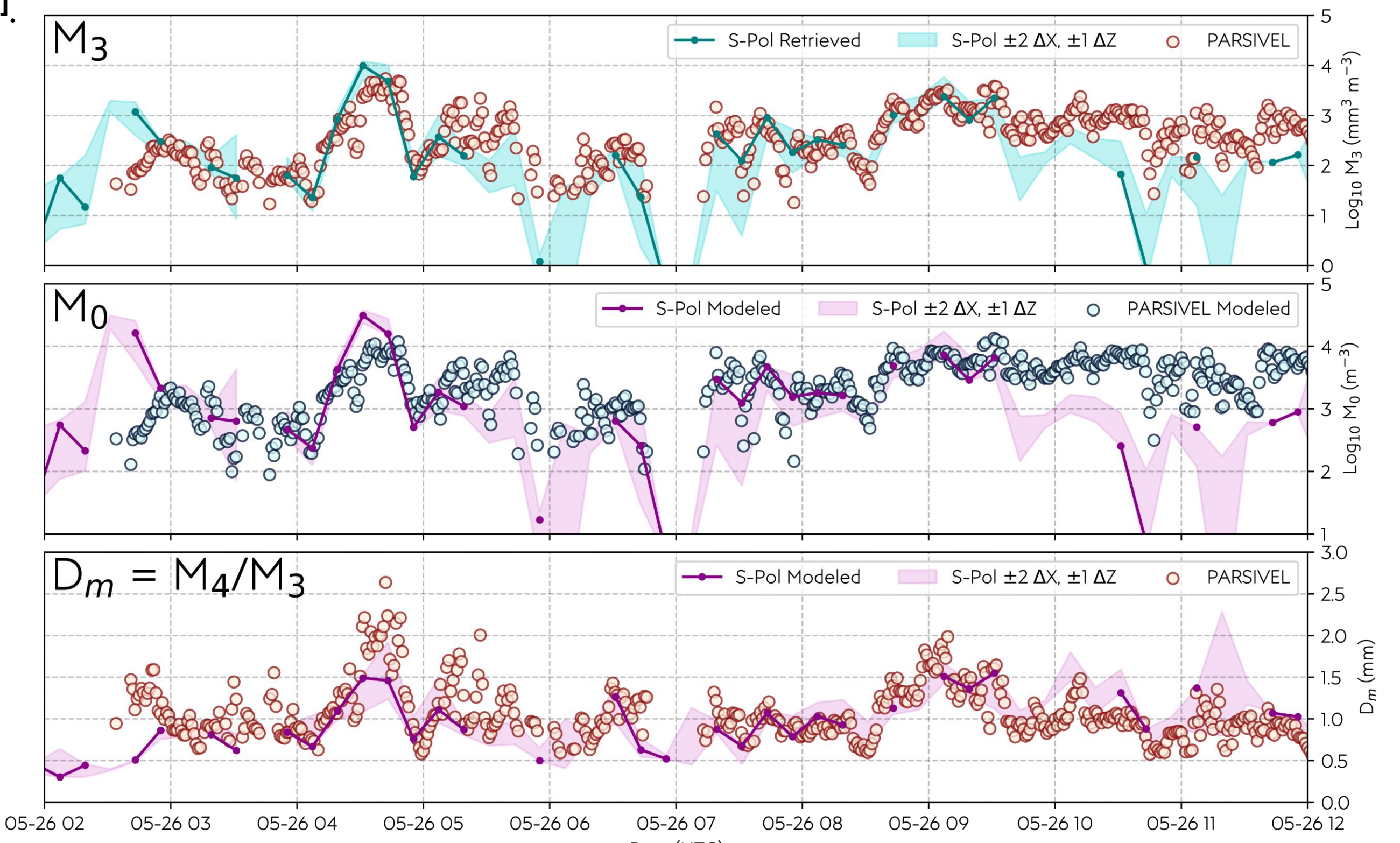


Figure 3: Retrieved and modeled M_3 , M_0 , and D_m using gridded S-Pol output 250 m above PRECIP PARSIVEL.

Links to Convective Ice Processes

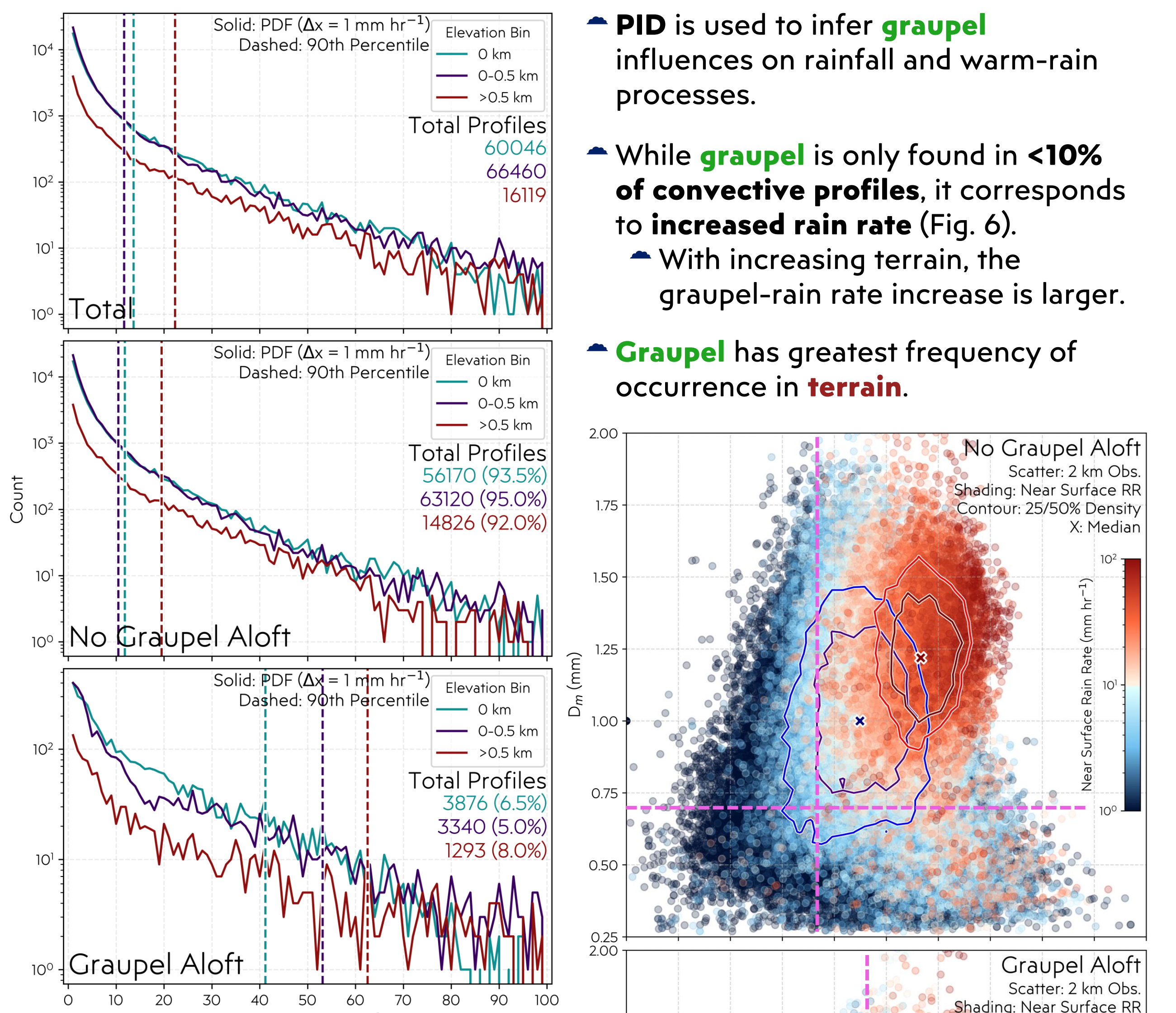


Figure 6: Distributions of near-surface rain rate with and without graupel aloft across elevation bins.

- PID** is used to infer **graupel** influences on rainfall and warm-rain processes.
- While **graupel** is only found in **<10% of convective profiles**, it corresponds to **increased rain rate** (Fig. 6).
 - With increasing terrain, the graupel-rain rate increase is larger.
- Graupel** has greatest frequency of occurrence in **terrain**.
- The impact of **graupel** on the DSD (M_0/D_m) in the context of rainfall is examined at 2-km height (Fig. 7).
- When **graupel** is present, **larger drops and more drop** are observed for a similar rain rate.
- To achieve **higher rain rates** (e.g., **>10 mm hr⁻¹**), a **minimum D_m and M_0 is required** and increases when graupel is present (**Dashed lines** in Fig. 7).

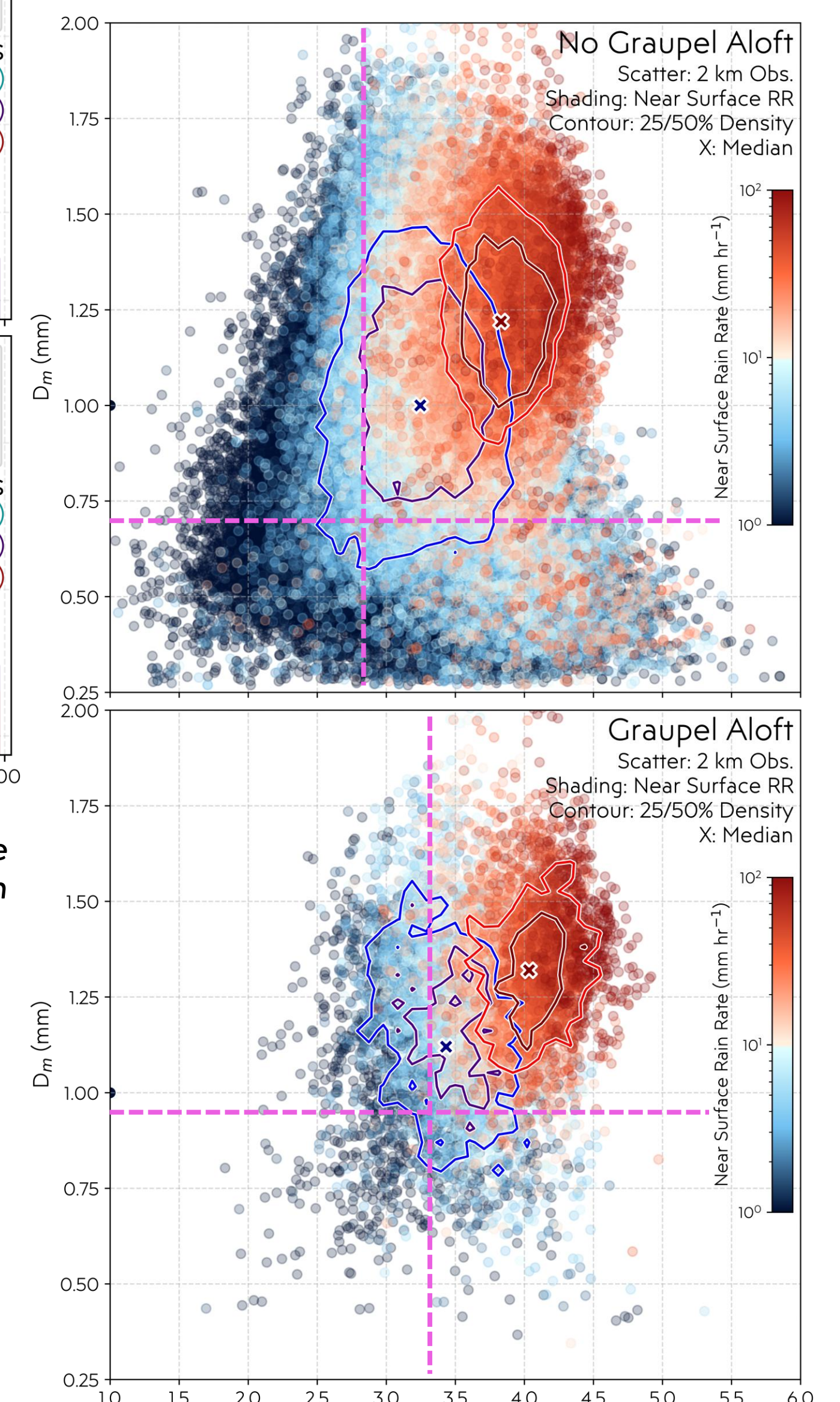


Figure 7: 2 km M_0/D_m phase space with near-surface rain rate with and without graupel aloft and subjective M_0/D_m minimum for >10 mm hr⁻¹ rain rates.

Key Findings

- Graupel** increases rain rate, particularly in **terrain**, through increasing **drop size and concentration**, as determined by **modeling DSDs**.

- To more accurately **model low-order moments**, training a DSD model with **complete DSDs** is required with a **combined MRR/2DVD** dataset being a valid candidate.
- The skill of a DSD model when applied to a radar is only as good as the **radar data quality**, therefore, great care is needed in processing the **radar data in terrain** considering **partial/complete beam blockage and ground clutter**.

References

- Cornejo et al. (2025) JTECH; DOI: 10.1175/JTECH-D-24-0094.1
- Lee et al. (2004) JAMC; DOI: 10.1175/1520-0450(2004)043<0264:AGATDN>2.0.CO;2
- Romatschke et al. (2022) JTECH; DOI: 10.1175/JTECH-D-22-0019.1
- Kumjian et al (2022) Rem. Sens.; DOI: 10.3390/rs14153706

Acknowledgements

This research is funded by NSF Award AGS-2146708

Contact

Ian Cornejo
 icornejo@wisc.edu

This research is currently under review at the Quarterly Journal of the Royal Meteorological Society

Pre-Print DOI: 10.22541/essoar.176617292.21587164/v2